

## Enhanced photoluminescence properties of $\text{Eu}^{3+}$ doped different phosphate glasses for red-orange light emission applications

B. NagarajaNaick\*, B. Deva Prasad Raju, Y. C. Ratnakaram

Department of Physics, Sri Venkateswara University, Tirupati 517502, India

\*Corresponding Author: B. NagarajaNaick, email: bukke.nag@gmail.com

**ABSTRACT:** Europium ( $\text{Eu}^{3+}$ ) ions doped different phosphate glasses having chemical compositions  $69.7 \text{NH}_4\text{H}_2\text{PO}_4 + 15\text{Na}_2\text{CO}_3 + 15\text{MCO}_3 + x\text{Eu}_2\text{O}_3$  (where  $x = 0.3$  and  $M = \text{Li}, \text{Mg}, \text{Ca}, \text{Sr}$  and  $\text{Ba}$ ) were prepared via standard melt quenching method. The prepared glasses were homogeneous and transparent. Structural characteristics were investigated through an XRD, FTIR, FT-Raman and solid state phosphorus-31 NMR spectroscopy. From FTIR and Raman spectra, structural units like triangular and tetrahedral-phosphates ( $\text{PO}_3$  and  $\text{PO}_4$ ) were found. Optical properties were designed by absorption (UV-Vis-NIR) and photoluminescence characterization (PL). Optical absorption from  ${}^7\text{F}_0$  and  ${}^7\text{F}_1$  states of the  $\text{Eu}^{3+}$ -doped different phosphate glasses has been studied to examine the covalent bonding characteristics using Judd-Ofelt ( $J-O$ ) intensity parameters. Various radiative parameters such as radiative transition probabilities ( $A_R$ ), effective bandwidths ( $\Delta\lambda_{\text{eff}}$ ), stimulated emission cross-sections ( $\sigma_{\text{emi}}$ ), experimental branching ratios ( $\beta_{\text{exp}}$ ) and radiative lifetimes ( $\tau_R$ ) etc. have been calculated and compared with other host glasses. The excitation spectra show strong intensity for  ${}^7\text{F}_0 \rightarrow {}^5\text{L}_6$  transition at 393 nm. Applying the 393 nm excitation wavelength, the luminescent emissions of  $\text{Eu}^{3+}$  doped samples have been analyzed. The chromaticity co-ordinates were also calculated from the photoluminescence spectra, which lie in the reddish region for all five glasses. Hence the obtained results suggest that present  $\text{Eu}^{3+}$ -doped different phosphate glasses are promising materials for reddish laser light applications.

**KEYWORDS:** Europium; Phosphate glass; FTIR;  ${}^{31}\text{P}$  NMR; Absorption; Photoluminescence

Date of Submission: 09-10-2020

Date of acceptance: 24-10-2020

### I. INTRODUCTION

In recent years, glasses doped rare earth (RE) ions are attracting attention since they are promising materials for high power laser applications. Rare earths doped phosphate materials are studied extensively due to their various applications in eco-friendly technology [1, 2]. They play important role in the improvement of display optical systems like cathode ray tubes, field emission displays, optoelectronic devices, temperature sensors and light emitting diodes [3-5]. These phosphate glasses were commercially manufactured for production of achromatic optical materials due to their low dispersion and low refractive index. Generally, the oxide glasses with alkali and alkaline earths are very much useful materials in optoelectronics and photonics. Adding of sodium oxide in the glass matrix will reduce its viscosity, melting temperature and also decrease the damage of the glass [6-8].

Among the RE ions, europium ( $\text{Eu}^{3+}$ ) is the remarkable activator for luminescent applications due to its attractive characteristics like intense red emission, simple energy level diagram and narrow emission in the UV-Vis region [9-11]. Oxide glasses doped with  $\text{Eu}^{3+}$  ions are extensively investigated for luminescent applications [12, 13]. Especially,  ${}^5\text{D}_0 \rightarrow {}^7\text{F}_2$  transition probability of  $\text{Eu}^{3+}$  is very sensitive to the chemical surroundings of  $\text{Eu}^{3+}$  ion and it has attracted a great amount of interest for applications [14].  $\text{Eu}^{3+}$  ion is used as one of the spectroscopic probes to investigate the local structure in host glasses [15]. Recently, Mithun et al. [16] reported improvement of red emission in  $\text{Eu}^{3+}$  doped  $\text{PbO-Na}_2\text{O-P}_2\text{O}_5$  glasses. Kindrat et al. [17] studied luminescence properties and quantum efficiency of the  $\text{Eu}^{3+}$ -doped borate glasses. Yamusa et al. [18] reported the  $\text{Eu}^{3+}$  ion impact on physical, optical and luminescent characteristics of barium sulfate borophosphate glasses. Gokce et al. [19] studied the characteristics of  $\text{Eu}^{3+}$  doped bismuth germanate glasses for red laser applications. Mariselvam et al. [20] reported the spectroscopic characteristics and Judd-Ofelt studies of  $\text{Eu}^{3+}$  doped barium bismuth fluoroborate glasses.

## II. EXPERIMENTAL DETAILS

### 2.1. Sample preparation

$\text{Eu}^{3+}$  doped different phosphate glasses were prepared using analar grade (AR) chemicals  $\text{NH}_4\text{H}_2\text{PO}_4$ ,  $\text{Na}_2\text{CO}_3$ ,  $\text{Li}_2\text{CO}_3$ ,  $\text{MgCO}_3$ ,  $\text{CaCO}_3$ ,  $\text{SrCO}_3$ ,  $\text{BaCO}_3$  and  $\text{Eu}_2\text{O}_3$  by using melt-quenching procedure. The purity of these chemicals is 99.99%. The details of preparation of the glass samples are explained in our earlier work [21]. The procured glass samples were used for spectral measurements. The details of the glass compositions are given below:

- (a) Li:  $69.7 \text{ NH}_4\text{H}_2\text{PO}_4 + 15\text{Na}_2\text{CO}_3 + 15\text{Li}_2\text{CO}_3 + 0.3\text{Eu}_2\text{O}_3$
- (b) Mg:  $69.7 \text{ NH}_4\text{H}_2\text{PO}_4 + 15\text{Na}_2\text{CO}_3 + 15\text{MgCO}_3 + 0.3\text{Eu}_2\text{O}_3$
- (c) Ca:  $69.7 \text{ NH}_4\text{H}_2\text{PO}_4 + 15\text{Na}_2\text{CO}_3 + 15\text{CaCO}_3 + 0.3\text{Eu}_2\text{O}_3$
- (d) Sr:  $69.7 \text{ NH}_4\text{H}_2\text{PO}_4 + 15\text{Na}_2\text{CO}_3 + 15\text{SrCO}_3 + 0.3\text{Eu}_2\text{O}_3$  and
- (e) Ba:  $69.7 \text{ NH}_4\text{H}_2\text{PO}_4 + 15\text{Na}_2\text{CO}_3 + 15\text{BaCO}_3 + 0.3\text{Eu}_2\text{O}_3$

### 2.2. Characterization

By using Archimedes' principle, the density of glasses were measured by immersing them in clean water and Abbe refractometer is used to determine the refractive indices of prepared glasses at sodium wavelength ( $589.3 \text{ nm}$ ). X-ray diffraction (XRD) profiles were obtained in the range  $10 - 70^\circ$  by using RIGAKU X-ray diffractometer to study the amorphous nature of glass. The FTIR spectra of glasses were recorded by BRUKER ALPHA 11 spectrometer in the range  $500$  to  $2500 \text{ cm}^{-1}$  with  $4 \text{ cm}^{-1}$  spectral resolution. The FT-Raman spectra of glass samples were analysed using BRUKER: RFS 27 spectrometer in the range  $0 - 4000 \text{ cm}^{-1}$ . Using JOEL ECX400 DELTA2 NMR spectrometer,  $^{31}\text{P}$  NMR spectra were recorded. The optical absorption studies were carried out in  $400 - 900 \text{ nm}$  range by using JASCO V-570 spectrophotometer. The excitation and emission measurements were attained by FLS - 980 spectrophotometer excited the samples by xenon source. All the optical measurements were performed at room temperature.

## III. RESULTS AND DISCUSSION

### 3.1. XRD analysis

The X-ray diffraction patterns of the prepared phosphate glasses are shown in Fig. 1 in the range of  $10^\circ \leq 2\theta \leq 70^\circ$ . The broadened peaks have been observed around  $25^\circ$  for all glasses and another peak is observed for Li and Mg glasses around  $40^\circ$  in the XRD spectrum. The XRD profiles of the studied glasses revealed broad haloes at lower angle side, it specifies the long range structural mutilate which is attributed to amorphous in nature.

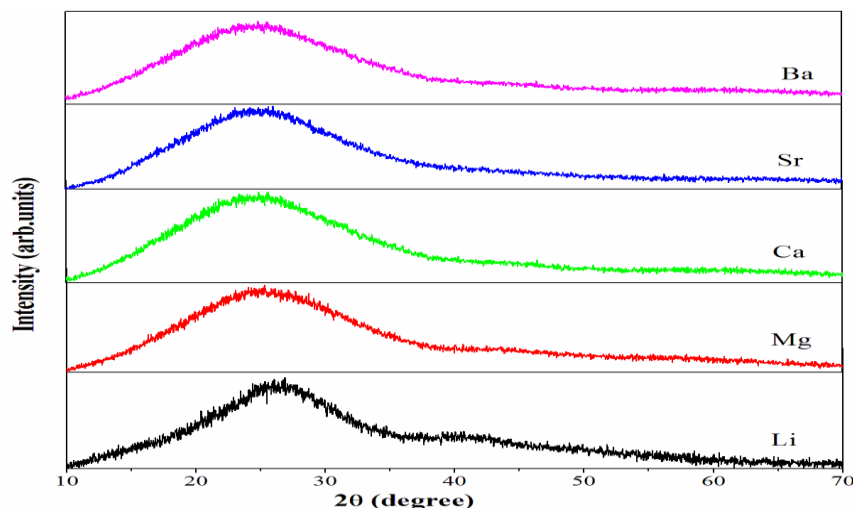
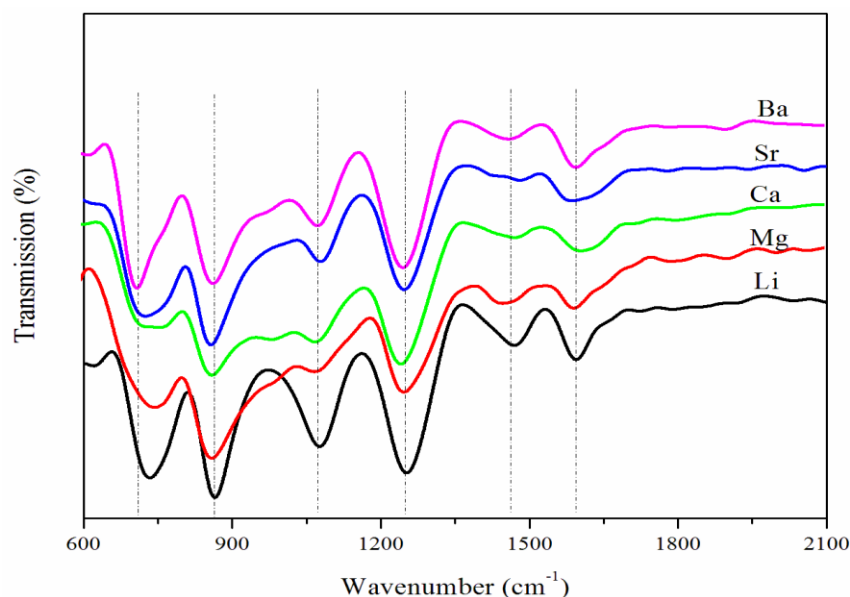


Fig. 1. XRD profiles of different phosphate glasses.

### 3.2. FTIR and FT-Raman analysis

The FTIR spectra have been charted in the scale  $600 - 2100 \text{ cm}^{-1}$  to analyze the functional groups and are shown in figure 2. The spectra consist of six bands appeared at  $\sim 750$ ,  $\sim 860$ ,  $\sim 1070$ ,  $\sim 1250$ ,  $\sim 1450$  and  $\sim 1590 \text{ cm}^{-1}$ . Band energies in respective five phosphate glass matrices along with their assignments are listed below.

Glass	Energy ( $\text{cm}^{-1}$ )	Assignment
Li, Mg, Ca, Sr and Ba	735, 736, 723, 731 and 706	symmetric stretching P-O-P units
Li, Mg, Ca, Sr and Ba	859, 861, 865, 852 and 863	asymmetric stretching P-O-P bridges [22]
Li, Mg, Ca, Sr and Ba	1079, 1073, 1073, 1075 and 1081	asymmetric stretching vibrations of P-O-P rings [23]
Li, Mg, Ca, Sr and Ba	1250, 1252, 1240, 1242 and 1244	asymmetric stretching vibrations mode of $\text{PO}_2$ groups [22]
Li, Mg, Ca, Sr and Ba	1480, 1440, 1472, 1487 and 1475	asymmetric stretching of $(\text{PO}_3)^{2-}$ terminal groups [24]
Li, Mg, Ca, Sr and Ba	1592, 1592, 1594, 1582 and 1590	C=C stretching Vibrations [25]



**Fig. 2.** FTIR spectra of 0.3mol% of  $\text{Eu}^{3+}$  doped different phosphate glasses.

Figure 3 represents the Raman spectra of  $\text{Eu}^{3+}$  doped different phosphate glasses. From the figure five vibrational bands are observed at about  $\sim 340$ ,  $\sim 530$ ,  $\sim 700$ ,  $\sim 1170$  and  $\sim 1250 \text{ cm}^{-1}$ . Appearance of these bands in prepared glasses suggested some changes in structural units in the phosphate network [28]. Assignments of different Raman peaks along with their energies with respect to five phosphate glasses are given below.

Glass	Energy( $\text{cm}^{-1}$ )	Assignment
Li, Mg, Ca, Sr and Ba	338, 340, 336, 338 and 340	$\text{PO}_3$ deformation vibrations of phosphate polyhedra [26]
Li, Mg, Ca, Sr and Ba	532, 527, 520, 525 and 521	O-P-O units and $\text{PO}_2$ modes of bending vibrations [27]
Li, Mg, Ca, Sr and Ba	700, 704, 696, 698 and 694	P-O-P group symmetric stretching vibrations mode of binding oxygen
Li, Mg, Ca, Sr and Ba	1165, 1180, 1169, 1163 and 1159	P-O-P group of symmetric stretching vibrations [28]
Li, Mg, Ca, Sr and Ba	1258, 1267, 1256, 1246 and 1244	O-P-O group asymmetric stretching vibrations of non-bridging oxygen[29]

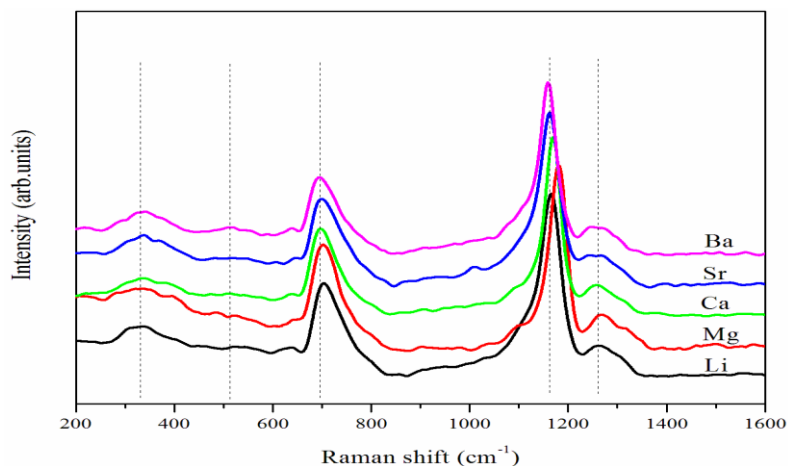


**Fig.3.** Raman spectra of 0.3mol% of  $\text{Eu}^{3+}$  doped different phosphate glasses.

### 3.3. Solid state $^{31}\text{P}$ NMR spectra

Solid state  $^{31}\text{P}$  NMR is a precious technique in analyzing the structures of phosphate-type glasses. Depending on the number of bridging oxygens per tetrahedron, the structure was discussed in our earlier studies [21, 23].  $^{31}\text{P}$  NMR spectra of  $\text{Eu}^{3+}$  doped five glasses were shown in Fig. 4. It is noticed from the figure that for the five studied glass samples, the prime signals with chemical shifts are shown at -21.03, -23.43, -22.91, -21.38 and -20.86 ppm for Li, Mg, Ca, Sr and Ba glasses respectively and these are related to metaphosphate structural units ( $\text{Q}^2$ ).

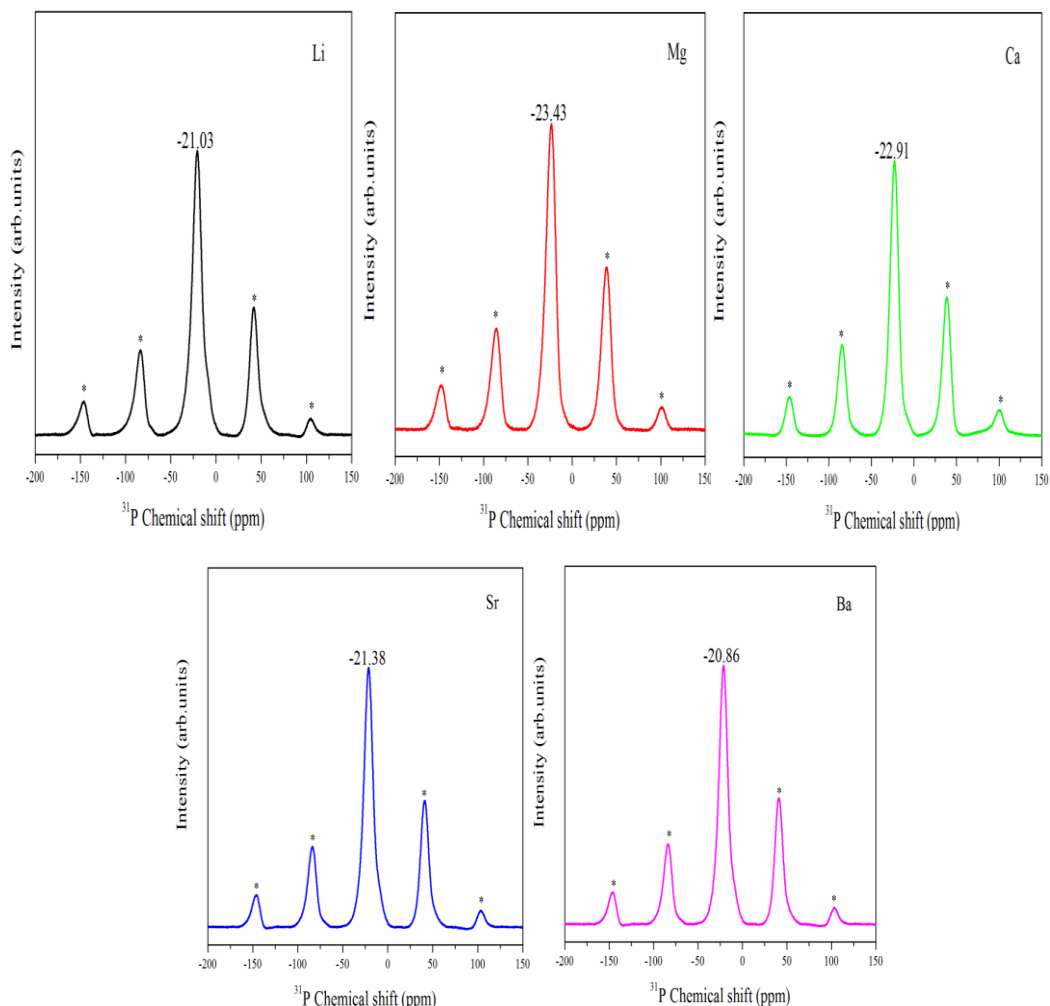


**Fig. 4.**  $^{31}\text{P}$  NMR spectra of 0.3mol%  $\text{Eu}^{3+}$  doped Li, Mg, Ca, Sr and Ba phosphate glasses.

### 3.4. Optical absorption spectra

Optical absorption spectra were taken in the UV-Visible region for all the studied samples at room temperature. We have observed seven absorption bands arise owing to the transitions from the ground multiplet  $^7\text{F}_0$  as well as  $^7\text{F}_1$  to different excited states as shown in Figure 5.

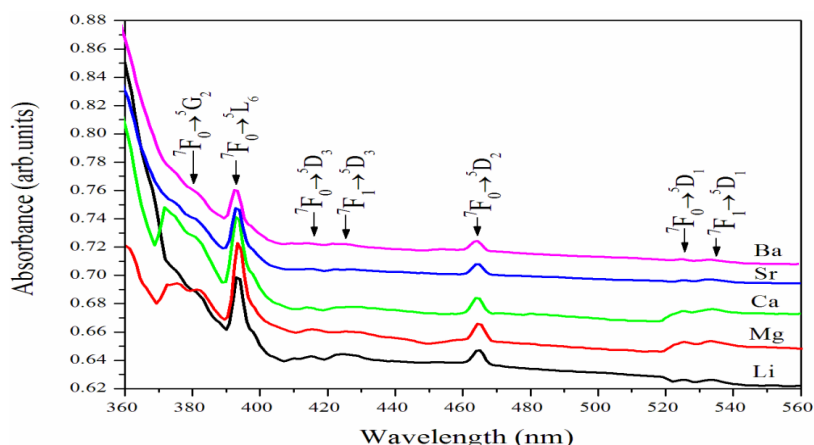


**Fig. 5.** UV-Visible absorption spectra of  $\text{Eu}^{3+}$  doped different phosphate glasses.

These absorption bands are ascribed to 4f-4f transition and in the present work, observed bands are due to the  $^7\text{F}_0 \rightarrow ^5\text{G}_2$ ,  $^7\text{F}_0 \rightarrow ^5\text{L}_6$ ,  $^7\text{F}_0 \rightarrow ^5\text{D}_3$ ,  $^7\text{F}_1 \rightarrow ^5\text{D}_3$ ,  $^7\text{F}_0 \rightarrow ^5\text{D}_2$ ,  $^7\text{F}_0 \rightarrow ^5\text{D}_1$  and  $^7\text{F}_1 \rightarrow ^5\text{D}_1$  for all the five glasses and these assignments were made based on Carnal et al. [30, 31]. Europium is a versatile element among the rare earth elements because, its transition  $^5\text{D}_0 \rightarrow ^7\text{F}_1$  is a magnetic dipole transition and it is independent of its environment. This transition can also be taken as reference for the transition from  $^5\text{D}_0$  level. The transitions below 350 nm cannot be resolved because the absorption edge of glass samples rises rapidly and obscure the  $\text{Eu}^{3+}$  ion upper energy level. In the present work  $^7\text{F}_0 \rightarrow ^5\text{L}_6$  is more intense transition; it is allowed by  $\Delta J$  selection rule but forbidden by  $\Delta L$  and  $\Delta S$  selection rule [32]. In the present glass  $^7\text{F}_0 \rightarrow ^5\text{D}_0$  (spin forbidden) transition is not observed because it is very weak in intense [33]. It is observed that,  $^7\text{F}_0 \rightarrow ^5\text{D}_2$  is more intense than  $^7\text{F}_0 \rightarrow ^5\text{D}_1$  and they are located at 465 nm and 525 nm, respectively. Also,  $^7\text{F}_0 \rightarrow ^5\text{D}_2$  is magnetic-dipole allowed and  $^7\text{F}_0 \rightarrow ^5\text{D}_1$  is electric-dipole allowed transition. The energies of several absorption bands observed for all the glasses are listed in Table 1.

**Table 1.** Energies ( $\nu$ ) ( $\text{cm}^{-1}$ ) of observed absorption bands and their assignments of different excited levels 0.3mol% of  $\text{Eu}^{3+}$  doped different phosphate glasses.

Transition	Glass				
	Li	Mg	Ca	Sr	Ba
$^7\text{F}_0 \rightarrow ^5\text{G}_2$	26212.3	26212.3	26219.2	26212.3	26137.0
$^7\text{F}_0 \rightarrow ^5\text{L}_6$	25425.9	25413.0	25406.5	25413.0	25406.5
$^7\text{F}_0 \rightarrow ^5\text{D}_3$	24079.0	24061.6	24090.6	24061.6	24131.3
$^7\text{F}_1 \rightarrow ^5\text{D}_3$	23562.7	23331.8	23337.2	23386.3	23612.8
$^7\text{F}_0 \rightarrow ^5\text{D}_2$	21454.6	21533.2	21537.8	21542.4	21482.3
$^7\text{F}_0 \rightarrow ^5\text{D}_1$	19033.2	19007.8	19022.3	19004.2	19004.1
$^7\text{F}_1 \rightarrow ^5\text{D}_1$	18712.6	18744.1	18789.9	18744.1	18723.1

In the present work, the spectral intensities of different absorption bands of  $\text{Eu}^{3+}$  doped phosphate glasses were obtained experimentally ( $f_{\text{exp}}$ ) and also thermally corrected ( $f^{\text{th}}$ ) spectral intensities are computed using the expressions given in ref. [34]. These values are presented in Table 2. It is observed that among five phosphate glasses, for most of the transitions, the spectral intensities are higher in Mg phosphate and lower in Ca phosphate glasses. It indicates that the asymmetry and bonding of RE within the matrix in Mg phosphate glass is high.

**Table 2.** Experimental (f) and thermally corrected (f\*) spectral intensities of different absorption bands 0.3mol% of Eu<sup>3+</sup> doped different phosphate glasses.

Transition	Li		Mg		Ca		Sr		Ba	
	f	f*								
<sup>7</sup> F <sub>0</sub> → <sup>5</sup> G <sub>2</sub>	0.08	0.11	0.98	1.45	1.78	2.63	0.09	0.13	0.08	0.12
<sup>7</sup> F <sub>0</sub> → <sup>5</sup> L <sub>6</sub>	1.65	2.44	2.08	3.08	1.91	2.83	1.90	2.81	1.42	2.10
<sup>7</sup> F <sub>0</sub> → <sup>5</sup> D <sub>3</sub>	0.12	0.17	0.07	0.10	0.04	0.05	0.05	0.07	0.05	0.08
<sup>7</sup> F <sub>1</sub> → <sup>5</sup> D <sub>3</sub>	0.25	0.82	0.10	0.33	0.15	0.50	0.11	0.37	0.13	0.44
<sup>7</sup> F <sub>0</sub> → <sup>5</sup> D <sub>2</sub>	0.25	0.37	0.31	0.45	0.27	0.39	0.23	0.34	0.26	0.39
<sup>7</sup> F <sub>0</sub> → <sup>5</sup> D <sub>1</sub>	0.03	0.04	0.08	0.12	0.07	0.10	0.02	0.02	0.02	0.03
<sup>7</sup> F <sub>1</sub> → <sup>5</sup> D <sub>1</sub>	0.06	0.20	0.06	0.20	0.05	0.15	0.08	0.26	0.06	0.20

### 3.5. Photoluminescence spectra

#### 3.5.1. Judd-Ofelt parameters and radiative properties

The variation of magnitudes of Judd-Ofelt (J-O) parameters ( $\Omega_\lambda$ ,  $\lambda = 2, 4$  and  $6$ ) with the variation of glass matrix suggests the variations in ligand fields around Eu<sup>3+</sup> sites in distinct glasses. J-O analysis has been taken to study the emission spectra using the emission transitions, <sup>5</sup>D<sub>0</sub>→<sup>7</sup>F<sub>2</sub> (for  $\Omega_2$ ) and <sup>5</sup>D<sub>0</sub>→<sup>7</sup>F<sub>4</sub> (for  $\Omega_4$ ) of Eu<sup>3+</sup> ion. The  $\Omega_6$  parameter could not be determined because the transition, <sup>5</sup>D<sub>0</sub>→<sup>7</sup>F<sub>6</sub> is not observed in the present work. Hence in this work, only the  $\Omega_2$  and  $\Omega_4$  parameters are determined for all the glass matrices and these values are presented in Table 3. It is noted that the magnitude of  $\Omega_2$  parameter is nearly same in all the five glasses studied and it is nearly  $1.6 \times 10^{-20}$  cm<sup>2</sup> indicating that not much variation in the covalence of Eu-O bond in these five glass matrices. Normally  $\Omega_4$  represents the rigidity and viscosity of the glass matrix. In the present work,  $\Omega_4$  is lower in Li glass and it is  $1.83 \times 10^{-20}$  cm<sup>2</sup> indicating lower rigidity and viscosity of the glass matrix. For the other four glass matrices, the magnitude of  $\Omega_4$  parameter is nearly same and it is  $3.0 \times 10^{-20}$  cm<sup>2</sup> indicating that there is not much change in the rigidity of the glass matrix. These values are compared with values reported in other glass matrices [35-38]. Among the four transitions, <sup>5</sup>D<sub>0</sub>→<sup>7</sup>F<sub>1</sub> transition is magnetic-dipole allowed, which is independent of the host glass, whereas, <sup>5</sup>D<sub>0</sub>→<sup>7</sup>F<sub>2</sub> and <sup>5</sup>D<sub>0</sub>→<sup>7</sup>F<sub>4</sub> transitions are impelled electric-dipole allowed and heavily depend on the host glass. This characteristic trend of the Eu<sup>3+</sup> allows the evaluation of J-O parameters from the emission spectra.

**Table 3.** Judd-Ofelt intensity parameters ( $\Omega_\lambda \times 10^{-20}$  cm<sup>2</sup>), luminescence intensity ratios (LIR) and their trends of Eu<sup>3+</sup> doped different phosphate glasses.

Glass	$\Omega_2$	$\Omega_4$	Trend	LIR	Reference
Li	1.60	1.87	$\Omega_4 > \Omega_2$	1.01	present work
Mg	1.59	3.08	$\Omega_4 > \Omega_2$	0.99	present work
Ca	1.58	3.09	$\Omega_4 > \Omega_2$	0.99	present work
Sr	1.59	3.05	$\Omega_4 > 2\Omega_2$	0.99	present work
Ba	1.60	3.00	$\Omega_4 > \Omega_2$	0.99	present work
ZBLAN:Eu <sup>3+</sup>	0.05	1.34	$\Omega_4 > \Omega_2$	-	[35]
KLa(PO <sub>3</sub> ) <sub>4</sub> :Eu <sup>3+</sup>	1.88	3.54	$\Omega_4 > \Omega_2$	-	[36]
BSYCaO-Eu <sup>3+</sup>	2.22	2.40	$\Omega_4 > \Omega_2$	-	[37]
PKALCaFEu	2.52	3.64	$\Omega_4 > \Omega_2$	0.96	[38]

The excitation spectrum of Eu<sup>3+</sup> doped lithium phosphate glass with an emission wavelength 624 nm is shown in Fig. 6. Figure 6 shows the six excitation peaks due to transitions, <sup>7</sup>F<sub>0</sub>→<sup>5</sup>D<sub>4</sub> (361nm), <sup>7</sup>F<sub>0</sub>→<sup>5</sup>G<sub>2</sub> (375nm), <sup>7</sup>F<sub>0</sub>→<sup>5</sup>L<sub>7</sub> (381nm), <sup>7</sup>F<sub>0</sub>→<sup>5</sup>L<sub>6</sub> (393nm), <sup>7</sup>F<sub>0</sub>→<sup>5</sup>D<sub>3</sub> (413nm) and <sup>7</sup>F<sub>0</sub>→<sup>5</sup>D<sub>2</sub> (563nm). From the spectra, it is seen that, the emission peak at 393 nm (<sup>7</sup>F<sub>0</sub>→<sup>5</sup>L<sub>6</sub>) is dominant. The emission spectra of Eu<sup>3+</sup> doped distinct phosphate glass matrices, under 393nm excitation have been recorded at RT and are shown in Fig. 7.

Spectra show five emission peaks relates to transitions, <sup>5</sup>D<sub>0</sub>→<sup>7</sup>F<sub>0</sub>, <sup>7</sup>F<sub>1</sub>, <sup>7</sup>F<sub>2</sub>, <sup>7</sup>F<sub>3</sub> and <sup>7</sup>F<sub>4</sub>. Among these five emission peaks, the peak relating to <sup>5</sup>D<sub>0</sub>→<sup>7</sup>F<sub>4</sub> transition is sharp and intense. The luminescence intensity ratio (LIR) between ED (electric dipole) and MD (magnetic dipole) transitions measures the symmetry of local environment of the Eu<sup>3+</sup> 4f sites. In the present work, for all glass matrices, the intensity of <sup>5</sup>D<sub>0</sub>→<sup>7</sup>F<sub>1</sub> (MD) transition is greater than <sup>5</sup>D<sub>0</sub>→<sup>7</sup>F<sub>2</sub> (ED) transition indicating symmetric nature present in all glass matrices. If this ratio is large, the rare earth ion is situated at lower site symmetry. The LIR values in different phosphate glass matrices are given in Table 2. From the table it is found that the LIR in Li glass is higher among five phosphate glasses and these ratios are equal in other four phosphate glasses. Thus Eu<sup>3+</sup> can be used as a probe for symmetric sites [39]. It is observed that, intensity of ED transition (<sup>5</sup>D<sub>0</sub>→<sup>7</sup>F<sub>2</sub>) increases when the symmetry

of  $\text{Eu}^{3+}$  site decreases. In this study, the intensity of the transition  $^5\text{D}_0 \rightarrow ^7\text{F}_2$  is decreasing in the order of  $\text{Mg} > \text{Li} > \text{Ca} > \text{Sr} > \text{Ba}$  in these phosphate glass matrices.

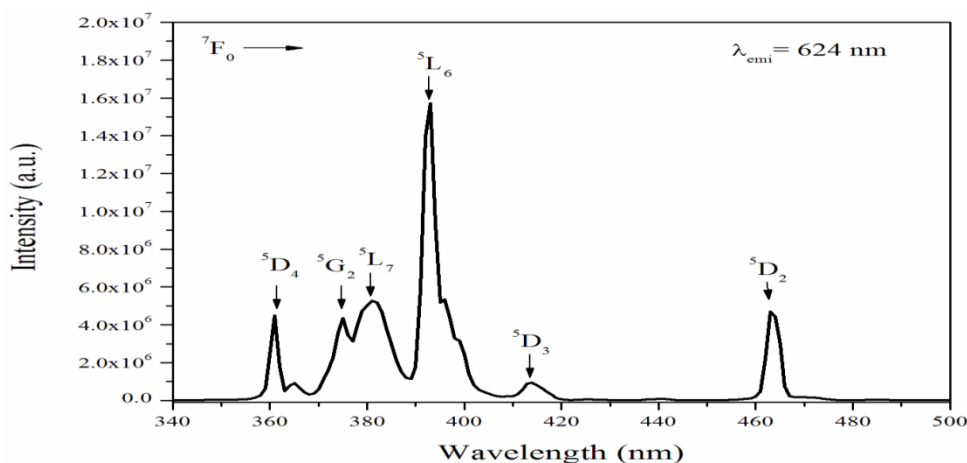


Fig. 6. Excitation spectrum of  $\text{Eu}^{3+}$  doped lithium phosphate glass.

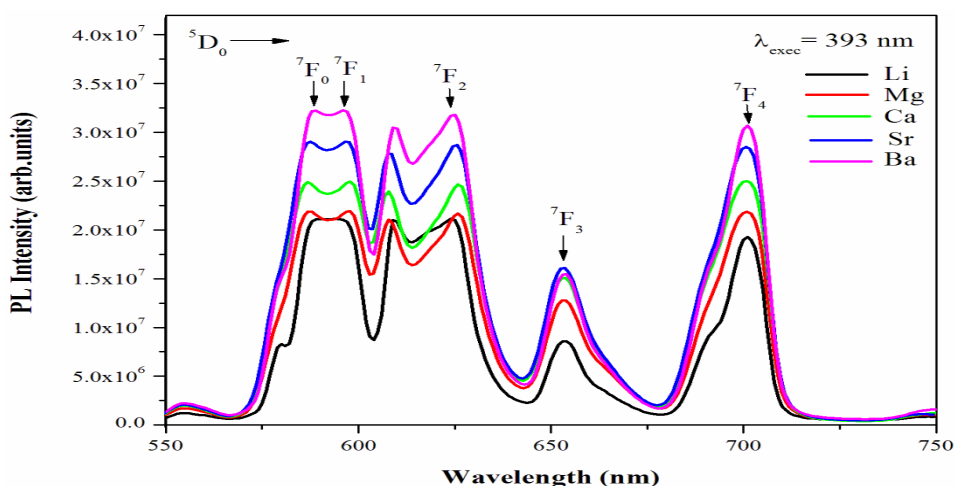


Fig. 7. Visible emission spectra of  $\text{Eu}^{3+}$  doped different phosphate glasses.

The obtained J-O parameters were used to evaluate  $A_R$  (radiative transition rates) and  $\tau_R$  (radiative lifetimes) for the excited level,  $^5\text{D}_0$  of  $\text{Eu}^{3+}$  doped distinct phosphate glasses and these values are tabulated in Table 4.

**Table 4.** Energies of transitions ( $\nu$ ,  $\text{cm}^{-1}$ ), Electric dipole transition ( $A_{ed}$ ,  $\text{S}^{-1}$ ), Magnetic dipole transition ( $A_{md}$ ,  $\text{S}^{-1}$ ), radiative transition probabilities ( $A_R$ ,  $\text{s}^{-1}$ ), total transition probabilities ( $A_T$ ,  $\text{S}^{-1}$ ) and radiative lifetimes ( $\tau_R$ ,  $\mu\text{s}$ ) for excited states of  $\text{Eu}^{3+}$  doped different phosphate glasses.

Glass	Transitions	$\nu$	$A_{ed}$	$A_{md}$	$A_R$	
Li	$^5\text{D}_0 \rightarrow ^7\text{F}_0$	17006.8	0	0	0	$A_T = 250.8$
	$^7\text{F}_1$	16806.7	0	61.52	61.52	$\tau_R = 3986$
	$^7\text{F}_2$	16025.6	62.06	53.34	115.40	
	$^7\text{F}_3$	15313.9	0	0	0	
	$^7\text{F}_4$	14265.3	36.32	37.62	73.94	
Mg	$^5\text{D}_0 \rightarrow ^7\text{F}_0$	17035.8	0	0	0	$A_T = 262.6$
	$^7\text{F}_1$	16722.4	0	59.39	59.39	$\tau_R = 3807$
	$^7\text{F}_2$	15974.4	57.56	51.77	109.33	
	$^7\text{F}_3$	15313.9	0	0	0	
	$^7\text{F}_4$	14265.3	57.03	36.86	93.89	
Ca	$^5\text{D}_0 \rightarrow ^7\text{F}_0$	17064.8	0	0	0	$A_T = 257.5$
	$^7\text{F}_1$	16722.4	0	58.48	58.48	$\tau_R = 3882$
	$^7\text{F}_2$	15974.4	54.86	50.98	105.84	
	$^7\text{F}_3$	15313.9	0	0	0	
	$^7\text{F}_4$	14265.3	56.91	36.31	93.22	

<b>Sr</b>	$^5\text{D}_0 \rightarrow ^7\text{F}_0$	17035.8	0	0	0	$A_T = 256.9$
	$^7\text{F}_1$	16722.4	0	58.20	58.20	$\tau_R = 3891$
	$^7\text{F}_2$	15974.4	56.39	50.74	107.13	
	$^7\text{F}_3$	15313.9	0	0	0	
	$^7\text{F}_4$	14265.3	55.50	36.13	91.63	
<b>Ba</b>	$^5\text{D}_0 \rightarrow ^7\text{F}_0$	17006.8	0	0	0	$A_T = 253.4$
	$^7\text{F}_1$	16750.4	0	57.68	57.68	$\tau_R = 3944$
	$^7\text{F}_2$	15974.4	55.88	50.03	105.91	
	$^7\text{F}_3$	15313.9	0	0	0	
	$^7\text{F}_4$	14265.3	54.27	35.63	89.90	

In this table,  $A_R$  (radiative transition probabilities),  $A_T$  (total transition probabilities) and  $\tau_R$  (radiative lifetimes) values were presented. It is noticed from the table that among five transitions ( $^5\text{D}_0 \rightarrow ^7\text{F}_0$ ,  $^7\text{F}_1$ ,  $^7\text{F}_2$ ,  $^7\text{F}_3$  and  $^7\text{F}_4$ ), the transition  $^5\text{D}_0 \rightarrow ^7\text{F}_2$  shows higher  $A_R$  value in Li glass and there is not much variation in  $A_R$  values for the remaining four phosphate glasses. It is also observed that radiative lifetimes ( $\tau_R$ ) of  $^5\text{D}_0$  state are increased slightly for Mg, Ca, Sr and Ba glasses and it is higher in Li glass.

The photoluminescence characteristics such as the emission peak wavelengths ( $\lambda_p$ ), effective bandwidths ( $\Delta\lambda_{\text{eff}}$ ), peak stimulated emission cross-sections ( $\sigma_{\text{emi}}$ ), optical gain bandwidths ( $\sigma_{\text{emi}} \times \Delta\lambda_{\text{eff}}$ ) and branching ratios ( $\beta_{\text{exp}}$  and  $\beta_{\text{cal}}$ ) of  $^5\text{D}_0$  state of different phosphate glasses were obtained using the standard expressions [41] and are presented in Table 5. From the table, it is observed that  $\Delta\lambda_{\text{eff}}$  are higher in Sr glass and lower in Mg glass for  $^5\text{D}_0 \rightarrow ^7\text{F}_2$  transition. It is also observed that the transition  $^5\text{D}_0 \rightarrow ^7\text{F}_2$  has higher branching ratios in Li glass and it is capable for laser emission.  $\beta_{\text{exp}}$  values are obtained from the relative areas of emission peaks. Generally emission cross-section ( $\sigma_{\text{emi}}$ ) is a significant parameter and is used to recognize the potential laser transition of RE ions in any host matrix. In the present work,  $\sigma_{\text{emi}}$  value is higher for transition  $^5\text{D}_0 \rightarrow ^7\text{F}_4$  in all the five glasses. Among the five glass matrices, Ba phosphate glass shows higher  $\sigma_{\text{emi}}$  value and it is better applicable for lasing material.

**Table 5.** Emission band positions ( $\lambda_p$ , nm), effective bandwidths ( $\Delta\lambda_{\text{eff}}$ ,  $\text{cm}^{-1}$ ), peak stimulated emission cross-sections ( $\sigma_e$ ,  $\times 10^{-22} \text{ cm}^2$ ), optical gain bandwidths ( $\sigma_e \times \Delta\lambda_{\text{eff}}$ ,  $\times 10^{-28} \text{ cm}^2$ ) and branching ratios ( $\beta_{\text{exp}}$  and  $\beta_{\text{cal}}$ ) of certain emission transitions of  $\text{Eu}^{3+}$  doped different phosphate glasses.

Glass	Transitions	$\lambda_p$	$\Delta\lambda_{\text{eff}}$	$\sigma_e$	$\sigma_e \times \Delta\lambda_{\text{eff}}$	$\beta_{\text{exp}}$	$\beta_{\text{cal}}$
<b>Li</b>	$^5\text{D}_0 \rightarrow ^7\text{F}_0$	588	345.7	0	0	0.213	0.000
	$^7\text{F}_1$	595	267.8	3.99	10.68	0.171	0.245
	$^7\text{F}_2$	624	495.8	4.45	22.06	0.349	0.460
	$^7\text{F}_3$	653	203.5	0	0	0.064	0.000
	$^7\text{F}_4$	701	386.2	4.62	17.84	0.203	0.295
<b>Mg</b>	$^5\text{D}_0 \rightarrow ^7\text{F}_0$	587	319.6	0	0	0.199	0.000
	$^7\text{F}_1$	598	231.6	4.10	9.49	0.150	0.226
	$^7\text{F}_2$	626	423.7	5.03	21.31	0.300	0.416
	$^7\text{F}_3$	653	203.1	0	0	0.093	0.000
	$^7\text{F}_4$	701	292.7	7.85	22.97	0.258	0.358
<b>Ca</b>	$^5\text{D}_0 \rightarrow ^7\text{F}_0$	586	314.2	0	0	0.181	0.000
	$^7\text{F}_1$	598	252.4	4.16	10.49	0.152	0.227
	$^7\text{F}_2$	626	496.4	4.20	20.84	0.325	0.411
	$^7\text{F}_3$	653	198.6	0	0	0.089	0.000
	$^7\text{F}_4$	701	307.4	7.49	24.28	0.253	0.362
<b>Sr</b>	$^5\text{D}_0 \rightarrow ^7\text{F}_0$	587	330.6	0	0	0.191	0.000
	$^7\text{F}_1$	598	239.5	4.38	10.49	0.143	0.226
	$^7\text{F}_2$	626	525.8	4.03	21.27	0.344	0.417
	$^7\text{F}_3$	653	203.3	0	0	0.081	0.000
	$^7\text{F}_4$	701	298.9	7.60	22.71	0.241	0.357
<b>Ba</b>	$^5\text{D}_0 \rightarrow ^7\text{F}_0$	588	340.7	0	0	0.224	0.000
	$^7\text{F}_1$	597	164.0	6.38	10.46	0.111	0.228
	$^7\text{F}_2$	626	458.2	4.61	21.12	0.342	0.418
	$^7\text{F}_3$	653	193.8	0	0	0.079	0.000

${}^7\text{F}_4$	701	270.5	8.31	22.47	0.243	0.355
------------------	-----	-------	------	-------	-------	-------

### 3.5.2. CIE chromaticity color coordinates

The CIE colour coordinates of present phosphate glasses were shown in Fig. 8. Using the color coordinates, the emitting colour of the light was calculated by the formulae as given in Ref [41]. The color coordinate values are (0.518, 0.303), (0.487, 0.322), (0.498, 0.319), (0.506, 0.317) and (0.489, 0.311) for Li,

Ca, Mg, Sr and Ba phosphate glasses, respectively. From the CIE diagram, it can be mentioned that the emitted light colours represents the red region. So it can be mentioned that, these glasses may be utilized in reddish emitting light applications.

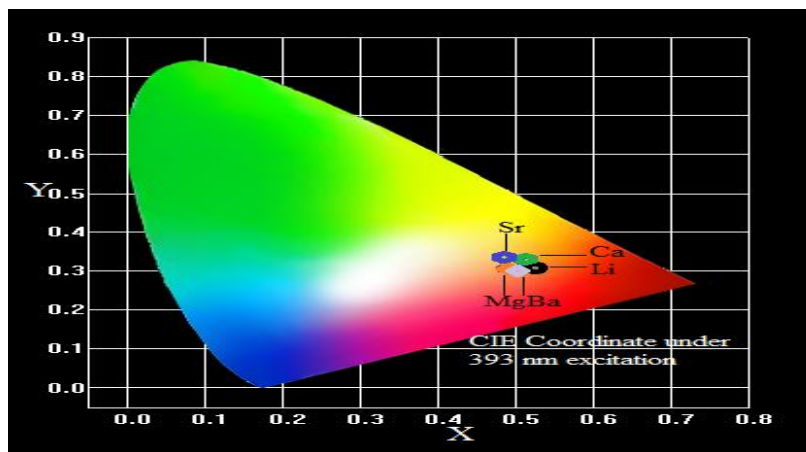


Fig. 8. CIE chromaticity diagram showing chromaticity coordinates (x, y) for  $\text{Eu}^{3+}$  doped different phosphate glasses.

## IV. CONCLUSIONS

0.3mol%  $\text{Eu}^{3+}$ -doped different phosphate glasses have been prepared by conventional melt quenching method. The structural and optical properties of these glasses have been designed by spectroscopic techniques. FTIR and FT-Raman spectra contain vibrational bands related to  $\text{PO}_3$  and  $\text{PO}_4$  structural units. The absorption spectra showed the existence of seven energy multiplets of  $\text{Eu}^{3+}$ . It is found that the transition  ${}^7\text{F}_0 \rightarrow {}^5\text{L}_6$  at 393 nm is very strong. Judd-Ofelt (J-O) theory was employed to examine the intensity parameters and radiative properties. Among the three J-O intensity parameters, the  $\Omega_2$  parameter was higher in Li phosphate glass and suggested to higher covalency and asymmetry in the glass matrix. Due to the absence of  ${}^5\text{D}_0 \rightarrow {}^7\text{F}_6$  transition in photoluminescence spectra,  $\Omega_6$  parameter values were not elucidated for all the glasses. The excitation spectra were recorded using excitation at 624 nm and it showed six peaks corresponding to six transitions and found that the high intensity peak was at 393 nm due to the transition  ${}^7\text{F}_0 \rightarrow {}^5\text{L}_6$ . From the emission spectra, five emission transitions were observed. Among the five emission transitions,  ${}^5\text{D}_0 \rightarrow {}^7\text{F}_2$  transition showed higher emission intensity, stimulated emission cross section and branching ratio values for all five glasses. Among all the phosphate glasses Li glass showed higher values which is suitable for reddish laser applications.

## ACKNOWLEDGEMENT

The author Prof. Y.C. Ratnakaram would like to thank University Grants Commission (UGC), New Delhi for the sanction of UGC-Mid career award.

## REFERENCES

- [1]. Ferhi M., Horchani-Naifer K., Hraiech S., Férid M., Guyot Y., Boulon G. Near infrared and charge transfer luminescence of trivalent ytterbium in  $\text{KLa}(\text{PO}_3)_4$  powders, *Opt. Commun.*, (2012) 285:2874–2878.
- [2]. Ehrtd. Structure, properties and applications of borate glasses, *Glass Technol.*, (2000) 41:182–185.
- [3]. Zhong J., Liang H., Han B., Su Q., Tao Y.  $\text{NaGd}(\text{PO}_3)_4:\text{Tb}^{3+}$  – A new promising green phosphor for PDPs application, *Chem. Phys. Lett.*, (2008) 453:192–196.
- [4]. Chen J.X.J., Cao G.S., Zhao X.B., Tu J.P., Zhu T.J. Electrochemical performance of  $\text{LiFe}_{1-x}\text{V}_x\text{PO}_4$ /carbon composites prepared by solid-state reaction, *J. Alloys Compd.*, (2008) 463:385–389.
- [5]. Chipaux R., Cribier M., Dujardin C., Garnier N., Guerassimova N., Mallet J., Meyer J.P., Pedrini C., Petrosyan A.G. Ytterbium-based scintillators, a new class of inorganic scintillators for solar neutrino spectroscopy, *Nucl. Instrum. Meth. Phys. Res. A*, (2002) 486:228–233.

- [6]. Silva G.H., Anjos V., Bell M.J.V., Carmo A.P., Pinheiro A.S., Dantas N.O.  $\text{Eu}^{3+}$  emission in phosphate glasses with high UV transparency, *J. Lumin.*, (2014)154:294–297.
- [7]. Sołtys M., Janek J., Zur L., Pisarska J., Pisarski W.A. Compositional-dependent europium-doped lead phosphate glasses and their spectroscopic properties, *Opt. Mater.*, (2015)40:91–96.
- [8]. Kiran N.  $\text{Eu}^{3+}$  ion doped sodium–lead borophosphate glasses for red light emission, *J. Mol. Struct.*, (2014)1065:93–98.
- [9]. Baldassare Di Bartolo (Ed.). *Advances in non-radiative processes in solids*, Plenum, New York, (1991)pp.282.
- [10]. Zaman F., Rooh G., Srisittipokakun N., Wongdeeying C., Kim H.J., Kaewkhao J. Physical, structural and luminescence investigation of  $\text{Eu}^{3+}$ -doped lithium-gadolinium bismuth-borate glasses for LEDs, *Solid State Sci.*, (2018)80:161–169.
- [11]. Kesavulu C.R., Kiran Kumar K., Vijaya N., Ki-Soo Lim, Jayasankar C.K. Thermal, vibrational and optical properties of  $\text{Eu}^{3+}$ -doped lead fluorophosphate glasses for red laser applications, *Mater. Chem. and Phys.*, (2013) 141:903–911.
- [12]. Bercher C., Riseberg L.A. Laser-induced fluorescence line-narrowing in rare-earth-doped glasses: Spectroscopic variations and their structural implications, *J. Non-Cryst. Solids*, (1980) 40:469–480.
- [13]. Powell R.C., Durville F.M., Behrens E.G., Dixon G.S. Four-wave mixing and fluorescence line narrowing studies of  $\text{Eu}^{3+}$  ions in glasses, *J. Lumin.*, (1988)40:68–71.
- [14]. Te-Hua Fang, Yee-Shin Chang, Liang-Wen Ji, Stephen D. Prior, Walter Water, Kuan-Jen Chen, Ching-Feng Fang, Chun-Nan Fang, Siu-T sen Shen. Photoluminescence characteristics of ZnO doped with  $\text{Eu}^{3+}$  powders, *J. Phys. Chem., Solids*, (2009) 70:1015–1018.
- [15]. Xavier Joseph, Rani George, Sunil Thomas, Manju Gopinath, Sajna M.S., Unnikrishnan N.V. Spectroscopic investigations on  $\text{Eu}^{3+}$  ions in Li–K–Zn fluorotellurite glasses, *Opt. Mater.*, (2014)37:552–560.
- [16]. Mithun De, Subhash Sharma, Samar Jana. Enhancement of  $^5\text{D}_0 \rightarrow ^7\text{F}_2$  red emission of  $\text{Eu}^{3+}$  incorporated in lead sodium phosphate glass matrix, *Physica B: Condens. Matter.*, (2019)556:131–135.
- [17]. Kindrat I.I., Padlyak B.V. Luminescence properties and quantum efficiency of the Eu-doped borate glasses, *Opt. Mater.*, (2018)77:93–103.
- [18]. Yamusa Y.A., Rosli Hussin, Wan Shamsuri W.N., Tanko Y.A., Siti Aisha Jupri. Impact of  $\text{Eu}^{3+}$  on the luminescent, physical and optical properties of  $\text{BaSO}_4 - \text{B}_2\text{O}_3 - \text{P}_2\text{O}_5$  glasses, *Optik*, (2018)164:324–334.
- [19]. Melis Gokce. Development of  $\text{Eu}^{3+}$  doped bismuth germinate glasses for red laser applications, *J. Non-Cryst. Solids*, (2019)505:272–278.
- [20]. Mariselvam K., Arun Kumara R., Jagadeesh M. Spectroscopic properties and Judd-Ofelt analysis of  $\text{Eu}^{3+}$  doped barium bismuth fluoroborate glasses, *Opt. Mater.*, (2018)84:427–435.
- [21]. Nagaraja Naick B., Reddy Prasad V., Damodaraiah S., Reddy A.V., Ratnakaram Y.C. Absorption and luminescence studies of  $\text{Sm}^{3+}$  ions activated in distinct phosphate glasses for reddish orange light applications, *Opt. Mater.*, (2019)88:7–14.
- [22]. Tiwari B., Pandey M., Sudarsan V., Deb S.K., Kothiyal G.P. Study of structural modification of sodium alumino phosphate glasses with  $\text{TiO}_2$  addition through Raman and NMR spectroscopy, *Physica B: Condens. Matter.*, (2009)404:47–51.
- [23]. Nagaraja Naick B., Damodaraiah S., Nagabhushana H., Ratnakaram Y.C. Effect of Li, Mg and Sr on structural and photoluminescence properties of  $\text{Nd}^{3+}$ -doped phosphate glasses for laser applications, *Phys. Chem. Glasses: Eur. J. Glass Sci. Technol.*, (2020)61:80–90.
- [24]. Pin-Yu shig, Han-Min shiu. Properties and structural investigations of UV-transmitting vitreous strontium zinc metaphosphate, *Mater. Chem. and Phys.*, (2007)106:222–226.
- [25]. Frank F Sene, Jose R, Martinelli, Emico Okuno. Synthesis and characterization of phosphate glass microspheres for radiotherapy applications, *J. Non-Cryst. Solids*, (2008)354:4887–4894.
- [26]. Koo J., Bae B.S., Na H. Raman spectroscopy of copper phosphate glasses, *J. Non-Cryst. Solids*, (1997)212:173–179.
- [27]. Elbatal H.A., Abdelghany A.M., ElBatal F.H., ElBadry Kh.M., Moustaff F.A. UV-visible and infrared absorption spectra of gamma irradiated CuO-doped lithium phosphate, lead phosphate and zinc phosphate glasses: A comparative study, *Physica B: Condens. Matter.*, (2011)406:3694–3703.
- [28]. Shajan D., Murugasen P., Sagadevan S. Studies on structural, optical and spectral properties of europium oxide doped phosphate glasses, *Optik*, (2017)136:165–171.
- [29]. Vijaya N., Jayasankar C.K. Structural and spectroscopic properties of  $\text{Eu}^{3+}$ -doped zinc fluorophosphate glasses, *J. Mol. Struct.*, (2012)1036:42–50.
- [30]. Dwivedi A., Joshi C., Rai S.B. Effect of heat treatment on structural, thermal and optical properties of  $\text{Eu}^{3+}$  doped tellurite glass: formation of glass-ceramic and ceramics, *Opt. Mater.*, (2015)45:202–208.
- [31]. Carnall W.T., Fields P.R., Rajnak K. Electronic energy levels in the trivalent lanthanide aquo ions. I.  $\text{Pr}^{3+}$ ,  $\text{Nd}^{3+}$ ,  $\text{Pm}^{3+}$ ,  $\text{Sm}^{3+}$ ,  $\text{Dy}^{3+}$ ,  $\text{Ho}^{3+}$ ,  $\text{Er}^{3+}$ , and  $\text{Tm}^{3+}$ , *J. Chem. Phys.*, (1968)49:4424–4442.
- [32]. Pavani K., Suresh Kumar J., Chengaiah T., Rama Moorthy L. Photoluminescence characteristics of  $\text{Eu}_2\text{O}_3$  doped calcium fluoroborate glasses, *J. Mol. Struct.*, (2012)1028:170–175.
- [33]. Hima Bindu S., Siva Raju D., Vinay Krishna V., Rajavardhana Rao T., Veerabrahmam K., Linga Raju Ch. UV light induced red emission in  $\text{Eu}^{3+}$ -doped zinc borophosphate glasses, *Opt. Mater.*, (2016)62:655–665.
- [34]. Ciric A., Stojadinovic S., Dramicanin M. DLuminescence intensity ratio thermometry and Judd-Ofelt analysis of  $\text{TiO}_2:\text{Eu}^{3+}$ , *Opt. Mater.*, (2018)85:261–266.
- [35]. McDougall J., Hollis D.B., Payne M.J.B. Judd-Ofelt parameters of rare earth ions in Zblali, ZBLAN and Zblak fluoride glasses, *Phys. Chem. Glass*, (1994)35:258–259.
- [36]. Ferhi M., Bouzidi C., Horchani-Naifer K., Elhouichet H., Ferid M. Judd-Ofelt analysis and radiative properties of  $\text{LiLa}_{(1-x)}\text{Eu}_x(\text{PO}_3)_4$ , *Opt. Mater.*, 2014, 37, P.607–613.
- [37]. Aryal P., Kesavulu C.R., Kim H.J., Lee S.W., Sang Jun Kang, Kaewkhao J., Chanthima N., Damde B. Optical and luminescence characteristics of  $\text{Eu}^{3+}$ -doped  $\text{B}_2\text{O}_3:\text{SiO}_2:\text{Y}_2\text{O}_3:\text{CaO}$  glasses for visible red laser and scintillation material applications, *J. Rare Earths*, (2018)36:482–491.
- [38]. Arun Kumar S., Marimuthu K. Structural and luminescence studies on  $\text{Eu}^{3+}:\text{B}_2\text{O}_3-\text{Li}_2\text{O}-\text{MO}-\text{LiF}$  ( $\text{M} = \text{Ba}, \text{Bi}_2, \text{Cd}, \text{Pb}, \text{Sr}_2$  and  $\text{Zn}$ ) glasses, *J. Lumin.*, (2013)139:6–15.
- [39]. Patra A., Sominska E., Ramesh S., Koltypin Yu., Zhong Z., Minti H., Reisfeld R., Gedanken A. Sonochemical preparation and characterization of  $\text{Eu}_2\text{O}_3$  and  $\text{Tb}_2\text{O}_3$  doped in and coated on silica and alumina nanoparticles, *J. Phys. Chem. B*, (1999)103:3361–3365.
- [40]. Sajna M.S., Subash Gopi, Prakashan V.P., Sanu M.S., Cyriac Joseph, Biju P.R., Unnikrishnan N.V. Spectroscopic investigations and phonon side band analysis of  $\text{Eu}^{3+}$ -doped multi-component tellurite glasses, *Opt. Mater.*, (2017)70:31–40.
- [41]. Nagaraja Naick B., Damodaraiah S., Reddy Prasad V., Vijaya Lakshmi R.P., Ratnakaram Y.C. Judd-Ofelt analysis and luminescence studies on  $\text{Dy}^{3+}$  doped different phosphate glasses for white light emitting material applications, *Optik*, (2019), 192:162980.